

## Perspectives on the Effect of Water in Cobalt Fischer-Tropsch Synthesis

---

Erling Rytter <sup>a, b</sup> and Anders Holmen <sup>a, \*</sup>

<sup>a</sup> Department of Chemical Engineering, Norwegian University of Science and Technology (NTNU), Sem Sæland vei 4, NO-7491 Trondheim, Norway

<sup>b</sup> SINTEF Materials and Chemistry, NO-7465 Trondheim, Norway

[\\*anders.holmen@ntnu.no](mailto:anders.holmen@ntnu.no)

### Abstract

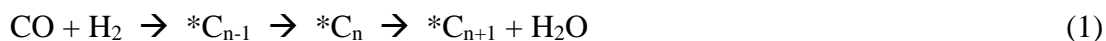
Water is an inherent component in Fischer-Tropsch Synthesis on Co catalysts and the impact of water is discussed with emphasis on alumina and aluminates. Water may affect the selectivity, activity, deactivation and state of the catalyst and, without exception, water is known to enhance the C<sub>5+</sub> selectivity by increasing the chain propagation  $\alpha$ -value. The effect of water depends on the catalyst. Small pore  $\gamma$ -Al<sub>2</sub>O<sub>3</sub> is less efficient at high water content than large pore  $\gamma$ -Al<sub>2</sub>O<sub>3</sub>. The effect of water on selectivity is independent of its origin, *i.e.* adding water to the feed has the same effect as water produced by the reaction. Arguments are provided for the effect of water being partly mechanistic in nature and occasionally due to pore condensation. In particular, we introduce *water assisted CO activation to methylidyne* as an option for generation of polymerization monomers. An additional factor that needs to be considered is that high water partial pressure is concurrent with reduction in hydrogen partial pressure. The influence of water strongly depends on the type of reactor employed.

### Keywords

Fischer-Tropsch Synthesis; Co catalysts; Effect of water; Al<sub>2</sub>O<sub>3</sub> support; CO activation

## Introduction

It is well known that water has a profound effect on many aspects of Fischer-Tropsch Synthesis (FTS), including selectivity, activity, deactivation and state of the catalyst.<sup>1</sup> The most striking effect of water is on the selectivity, *i.e.* selectivity depends on the conversion level.<sup>2</sup> Many reports are unfortunately based on constant GHSV (Gas Hourly Space Velocity) instead of constant conversion, making conclusions on chain growth difficult or impossible. Water is an inherent component in FTS as one water molecule is generated for each molecule of CO that is converted:



where the star signifies that a hydrocarbon chain is attached to atoms on the active cobalt surface. Termination can take place for each chain length by hydrogenation of the chain end or by hydrogen abstraction ( $\beta$ -hydrogen elimination) giving paraffins or olefins, respectively. If carbon selectivity is known for each carbon number over a wide range, the polymerization probability  $\alpha$  can be derived from the Anderson-Schultz-Flory (ASF) relationship:<sup>3</sup>

$$W_n = n (1-\alpha)^2 \alpha^{n-1} \quad (2)$$

where  $W_n$  is the weight fraction of hydrocarbon with chain length  $n$  and  $\alpha$  is defined by

$$\alpha = R_p / (R_p + R_t) \quad (3)$$

with  $R_p$  and  $R_t$  being the propagation and termination rates, respectively, of chain growth.

Several theories and mechanistic explanations have been offered to explain the influence of water in FTS. One hypothesis is that higher water partial pressure suppresses hydrogenation reactions at the surface, *e.g.* by occupying hydrogen sites.<sup>4</sup> This model is consistent with separate experiments on propene hydrogenation.<sup>5</sup> Krishnamoorthy *et al.* suggested for Co/SiO<sub>2</sub> catalysts that increased reaction rates were due to water influence on the active species distribution on the cobalt surface.<sup>6</sup> This is in line with the Steady-State Isotopic Transient Kinetic Analysis (SSITKA) study of Bertole *et al.* of Co and CoRe on TiO<sub>2</sub> where they found that adsorbed water accelerates the CO dissociation rate with subsequent formation of CH<sub>x</sub> monomers.<sup>7</sup> Co-adsorbed water presumably interacts with CO and lowers the energy barrier for CO activation. Similarly, increase in C<sub>5+</sub> was associated with increased coverage of reactive monomer species resulting in higher polymerization rate without a simultaneous effect on termination probability. The previous suggestion of water enhancement in syngas diffusion rate seems to have been disproved,<sup>8</sup> and it is now likely that it is the active CH<sub>x</sub> carbon inventory that is the key factor. Fischer *et al.* opened up for water-induced changes of the active sites responsible for chain growth or by an inhibiting effect of water on methanation sites.<sup>9</sup> For the present analysis we find it unnecessary to make a distinction between polymerization and methanation sites as there is a mechanistic link between these reactions in Fischer-Tropsch synthesis.<sup>4,10</sup> Hibbitts *et al.* studied how the water pressure influences FTS on ruthenium catalysts and deduced mechanistic insight through DFT calculations.<sup>11</sup> They concluded that H<sub>2</sub>O mediates H-transfer resulting in enhanced rate of CH<sub>x</sub> monomer formation and they

propose that the same holds for cobalt catalysts. The underlying nature of the enhancement effect of water on olefin selectivity has been studied recently on model reactions.<sup>12</sup>

The present work is concerned with all aspects of water in FTS, including consequences for industrial operations. The main part of the paper is based on experience gained at the Department of Chemical Engineering, NTNU, and Statoil Research Centre during the past 30 years.

### **Water levels in Fischer-Tropsch reactors**

It is useful to visualize the actual water levels in commercial and laboratory reactors by simple stoichiometry and taking into account possible condensation of water in the syngas feed and in the reactor itself. Two types of reactors are considered; slurry bubble columns and fixed-bed. The latter is divided into conventional tubular fixed-bed and microchannel reactors. The laboratory counterparts are continuously stirred tank reactors (CSTR) and micro-reactors; typically 0.5-2 L and diameter 3-10 mm, respectively.

Water levels are reported in three alternative ways; absolute partial pressure, the  $\text{H}_2\text{O}/\text{H}_2$  ratio, and  $\text{H}_2\text{O}/\text{CO}$ . Most relevant is probably the steam to hydrogen ratio as it reflects the propensity for cobalt oxidation versus reduction. At the same time water is known, without exception, to enhance  $\text{C}_{5+}$  selectivity by increasing the chain propagation  $\alpha$ -value while hydrogen may work in the opposite way, *i.e.* promoting chain termination. These effects were recently discussed in papers on deactivation and selectivity in FTS,<sup>4,13</sup> and are also analyzed later in the present work. The steam to carbon ratio is a well-known parameter in natural gas reforming as a certain steam level is required to avoid coking and carburization in feed lines, in the reactor, and in product cooling equipment.<sup>14</sup> It therefore seems interesting to look at the steam to CO ratio and investigate if any correlation can be inferred to long term deactivation by carbonaceous deposits. Another indication of the importance of  $\text{H}_2\text{O}/\text{C}$  is that catalytic gasification of biomass has been shown to take place in water at temperatures resembling FTS; so-called aqueous reforming.<sup>15</sup>

Calculated  $\text{H}_2\text{O}/\text{H}_2$  levels are shown in Figure 1 as a function of CO conversion. The result is strongly dependent on the  $\text{H}_2/\text{CO}$  ratio in the feed gas. For simplicity, we have assumed that the  $\text{H}_2/\text{CO}$  consumption ratio is 2.15, but actually this number varies somewhat with the  $\alpha$ -value. For syngas compositions with  $\text{H}_2/\text{CO}$  below 2.15, hydrogen is depleted in the gas as the reaction proceeds, and it is evident from the figure that this leads to a strong increase in  $\text{H}_2\text{O}/\text{H}_2$  for progressively lower CO conversions.

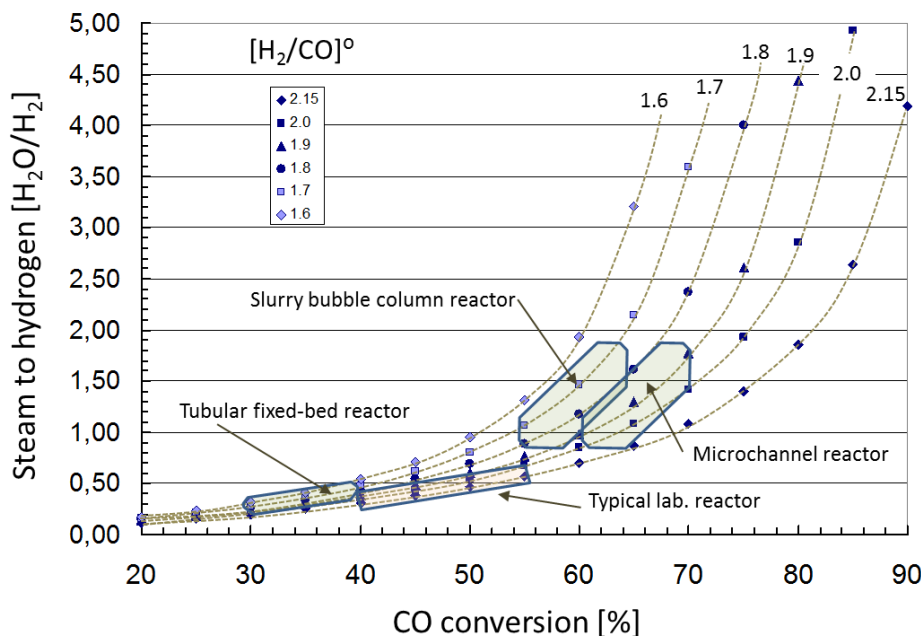
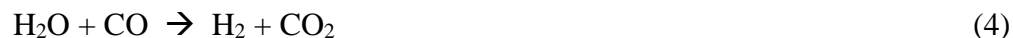


Figure 1. Steam to hydrogen ratio in Fischer-Tropsch synthesis as a function of CO conversion and syngas feed composition. Typical conditions for industrial reactors as well as laboratory reactors are indicated. Assumptions: dry syngas and constant  $H_2/CO$  consumption ratio of 2.15.

Four sections of the diagram are highlighted according to our experience; three that are relevant for commercial type reactors and one that is typical for laboratory reactors. Most research groups realize today the strong influence of conversion on selectivity and therefore constrain themselves to a fairly constant interval of conversions by adjusting GHSV; typically in the 40-55% CO conversion range. Simultaneously, the  $H_2/CO$  feed ratio is usually in the range 2.0 to 2.15. It is interesting to note that typical laboratory conditions are outside the operating range of all industrial applications. Fixed-bed reactors are characterized by a gradual increase in conversion from zero to the value at the outlet, and it is the latter conditions that are pinpointed in Figure 1. The conversion in tubular fixed-bed reactors, as practiced by Shell,<sup>16</sup> is limited by heat transfer. One interesting observation for moderate conversion levels is that there is full flexibility in adjusting the  $H_2/CO$  ratio in the syngas to as low level as is desired in order to improve  $C_{5+}$  selectivity. At the other extreme are the conditions reported for microchannel reactors.<sup>17</sup> Excellent heat control and near isothermal conditions have allowed comparably high CO conversions that approach and sometimes exceed 70%. High conversion comes at the expense of ability to reduce the hydrogen content in the feed gas in order to keep the steam level in a suitable range; say  $H_2O/H_2$  below 2. Slurry bubble column reactors are characterized by a vigorous flow pattern, rapid breaking and formation of bubbles, high degree of back-mixing in the fluid and gas, and efficient heat removal. Therefore, the gas composition is approaching the outlet composition and is fairly constant throughout the reactor volume. Constant gas composition is beneficial for selectivity, but the reaction rate is limited by a fairly high proportion of inerts;  $H_2O$ ,  $CH_4$  and  $CO_2$ . Very careful

reactor control is necessary to avoid high conversion levels. For example, if the GHSV is reduced during upsets in the syngas supply or during shut-down to allow a conversion of 75%, then the  $H_2O/H_2$  level increases to above 8 with potential serious damage to the catalyst. These conditions also favor the water-gas-shift (WGS) reaction:



giving high amounts of  $CO_2$ ; particularly if the catalyst becomes partly oxidized.

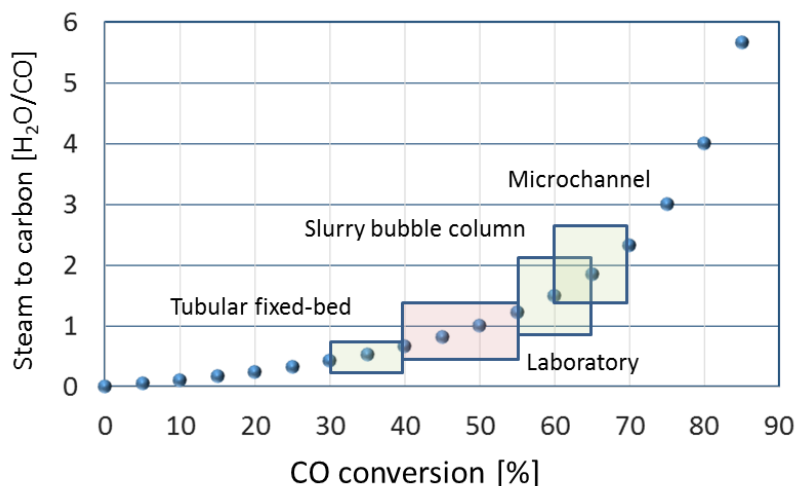


Figure 2. Steam to carbon ratio in Fischer-Tropsch synthesis as a function of CO conversion. Operating ranges for industrial type and laboratory reactors are indicated. Assumption: dry syngas.

The steam to carbon ratio (S/C) in terms of  $H_2O/CO$  is shown in Figure 2 for different CO conversion levels. Depending on the process at hand, often all kinds of hydrocarbons, and even  $CO_2$ , are included in the S/C ratio. Nevertheless, we regard CO as more relevant under FT conditions as it is CO that is the precursor to carbon species at the catalyst surface. Due to the stoichiometry of the FT reaction, Eq. 1, with one mole  $H_2O$  generated for each mole CO converted, the steam to carbon ratio is independent of  $H_2/CO$  in the feed. It is inferred from the diagram that slurry reactors might be more robust in terms of S/C as the fixed-bed reactor types operate from 0 conversion at the inlet to the conversions indicated in the boxes. If desired, however, water can be added to the feed; for instance as part of the recycle stream of unconverted syngas.

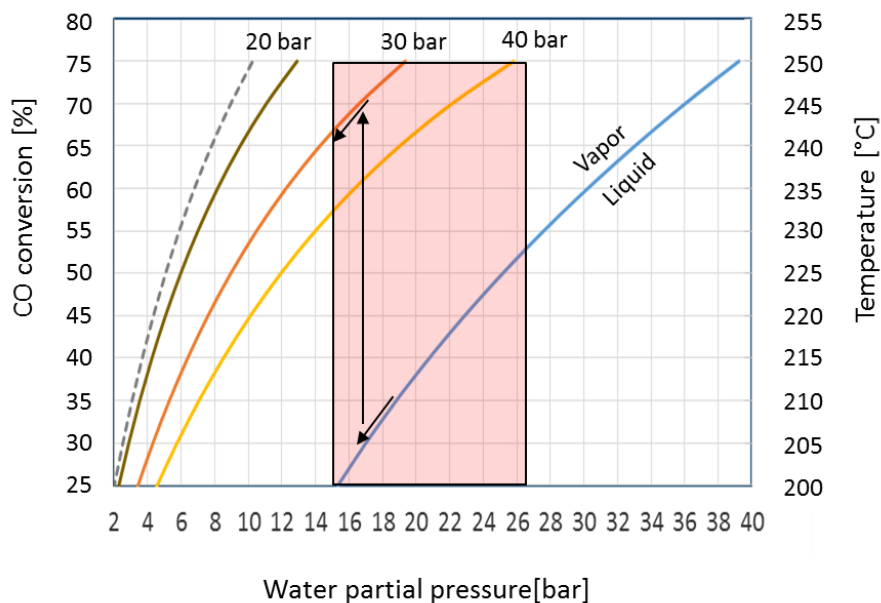


Figure 3. Water condensation pressure at different temperatures (blue line) compared to partial pressure of water during FT reaction for different conversion levels and total pressures. Assumptions:  $H_2/CO$  feed ratio of 1.7, except dotted line for 2.0; 10% of converted CO is gaseous hydrocarbons.

The condensation line for water vapor at different temperatures is given for the relevant FTS temperature range to the right in Figure 3. The left part shows the generated water vapor pressure by FTS as a function of CO conversion for different pressures and typical  $H_2/CO=1.7$  feed ratio for a slurry reactor. This implies that certain combinations of temperature, conversion and pressure in the shaded area lead to condensation. For example, taking into account 5 °C and 5% conversion safety margins, reaction at 210 °C and 30 bar is limited to 65% conversion; follow the black arrows in the figure. These restrictions imply that water condensation is prohibited. However, we are not aware of studies where water deliberately is condensed in a fixed-bed or slurry reactor and the consequences for FTS performance.

### Catalyst support and activity

There have been a large number of studies on the effect of added water on Fischer-Tropsch catalyst activity. A summary from 2007 gives 11 references to work on alumina supported cobalt catalysts, 9 to work on silica supported catalysts, and 5 to titania supported.<sup>1</sup> Both positive and negative responses were observed; mostly positive for titania and silica and mostly negative for  $\gamma$ -alumina. It has, however, been found that it is misleading to ascribe the water effect to the type of support alone as a distinct trend with pore size has been observed for both alumina and silica. Specifically, there is a clear distinction between medium and large pore  $\gamma$ -alumina.<sup>18,19</sup> The medium pore size catalyst has a negative response to water addition while the large pore one exhibits a positive response. This observation is in line with other supports where narrow to medium range  $\gamma$ -alumina

is unfavorable and silica, titania,  $\alpha$ -alumina and aluminates are favorable with respect to activity upon water addition.<sup>20,21,22</sup> The activity usually is restored to its anticipated trend from deactivation after the water feed is turned off, although this may take a few days.

Two further examples are given in Figure 4. The lower part of the figure shows how a Co on platelet carbon nanofiber (CNF) catalyst responds in periods where 3.0 or 6.3 bar water is added to the syngas feed; keeping the total pressure unchanged.<sup>23</sup> Even though the syngas pressure therefore is reduced, catalyst activity increases significantly in both periods. Simultaneously there is a considerable deactivation of the catalyst. Returning to initial syngas composition shows that the deactivation in this case is irreversible. The activity is far below the value found for a reference test with no water addition. All these CNF based catalysts have calculated narrow pores in the 6-8 nm range, and a positive response is therefore atypical. A somewhat different response is observed for a catalyst on nickel aluminate with metallic nickel as promoter.<sup>21</sup> Adding 3.0 bar water is highly successful; resulting in a period with high productivity and a deactivation rate as expected. Increasing the water pressure to 6.6 bar evidently is too much as seen from a drop in activity and an enhanced deactivation rate. After a test period with half the syngas pressure, the reaction rate returns to the expected deactivation profile. Ma *et al.* performed continuously stirred tank reactor (CSTR) experiments with a Co/Ru/Al<sub>2</sub>O<sub>3</sub> catalyst by adding 10% water to the syngas feed. A reversible positive kinetic effect was found in low conversion experiments where care was taken not to oxidize the active metal.<sup>24</sup>

It is concluded that:

- Adding limited amounts of water to the feed in Fischer-Tropsch synthesis usually increases catalyst activity. It is suggested that activation of CO is promoted by water giving higher concentration of propagation monomers. This model is in line with SSITKA studies under elevated pressure.<sup>7</sup> Rate constant per CH<sub>x</sub> specie is unchanged, but global rate constant increases when water is added.
- Adding large amounts of water results in loss of activity and a high deactivation rate that is reversible or irreversible depending on catalyst formulation. Narrow to medium pore size alumina and silica are particularly sensitive to water addition. This is suggested to be due to surface water condensation; possibly causing diffusion limitations of syngas.

Most published rate equations do not comprise water as a term, but there are five studies that present explicit Langmuir-Hinshelwood expressions;<sup>24,25,26,27,28</sup> all for different catalyst compositions. Only overall rates for CO conversion were given as no separation into formation of product groups was derived. Recent work has analyzed the response of the different rate expressions to variation in FTS conditions, in particular conversion and feed composition.<sup>29</sup> From the latter study it was concluded that the expressions are very different and may reflect variations in catalysts used, consistent with the water responses discussed above. For example, Davis *et al.* have developed alternative expressions that show positive or negative water effects

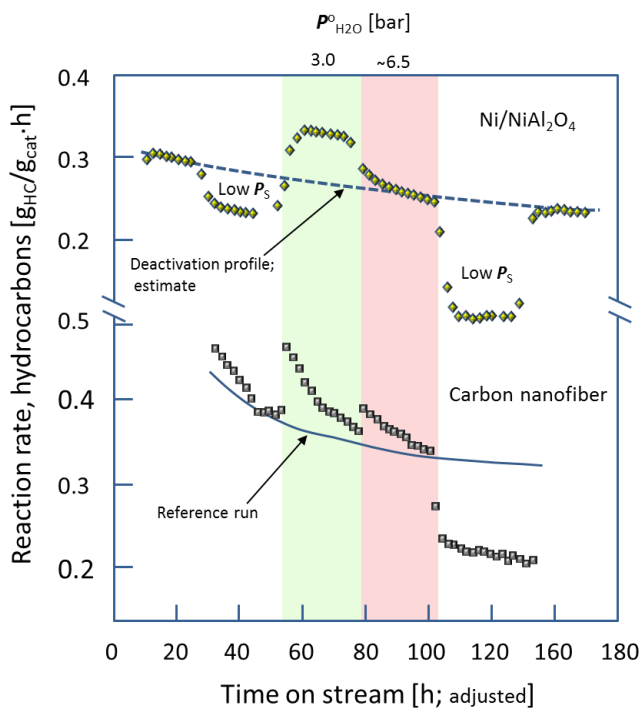


Figure 4. Reaction rate to hydrocarbons in experiments where water of 3.0 and 6.6 or 6.3 bar is added to syngas at 210 °C and 20 bar total pressure. Initial conversion is adjusted to ca. 50%. Upper part: 12 wt% Co/5 wt% Ni/NiAl<sub>2</sub>O<sub>4</sub> catalyst; ultra large pore: 13.3 m<sup>2</sup>/g, 60 nm; H<sub>2</sub>/CO = 2.0. in feed; two periods of 15 or 10 bar syngas pressure ( $P_S$ ) by adding He. Lower part: 12 wt% Co/Platelet CNF catalyst; narrow pore: 165 m<sup>2</sup>/g, 6.3 nm; H<sub>2</sub>/CO = 2.1. in feed. Replotted from literature.<sup>21,23</sup>

### Catalyst support and selectivity

Comparison of the effect of partial pressure of water for Co/Re catalysts on narrow, medium and wide pore  $\gamma$ -alumina is shown in Figure 5a. Dependency of pore size at all conditions is evident as is selectivity improvement upon adding water to syngas.<sup>18</sup> Figure 5b shows the same trend for catalysts on carbon nanofibers of the platelet type.<sup>23</sup> By impregnation from water or organic solvent, the Co crystallite size from hydrogen chemisorption was 18 and 8 nm, respectively. It is interesting that by adding water to syngas the trend from increasing conversion just continues; strongly supporting a model whereby the impact of water is independent of its origin. A similar conclusion was reached previously in a study on the water effect of Re promoted and unpromoted cobalt catalysts on titania, silica and alumina.<sup>22</sup> The parallelism of the stippled lines for medium and large pore alumina and both CNF samples indicates that the positive effect of water has the same origin for all these supports; with the exception for narrow pore  $\gamma$ -alumina standing out as the least efficient.



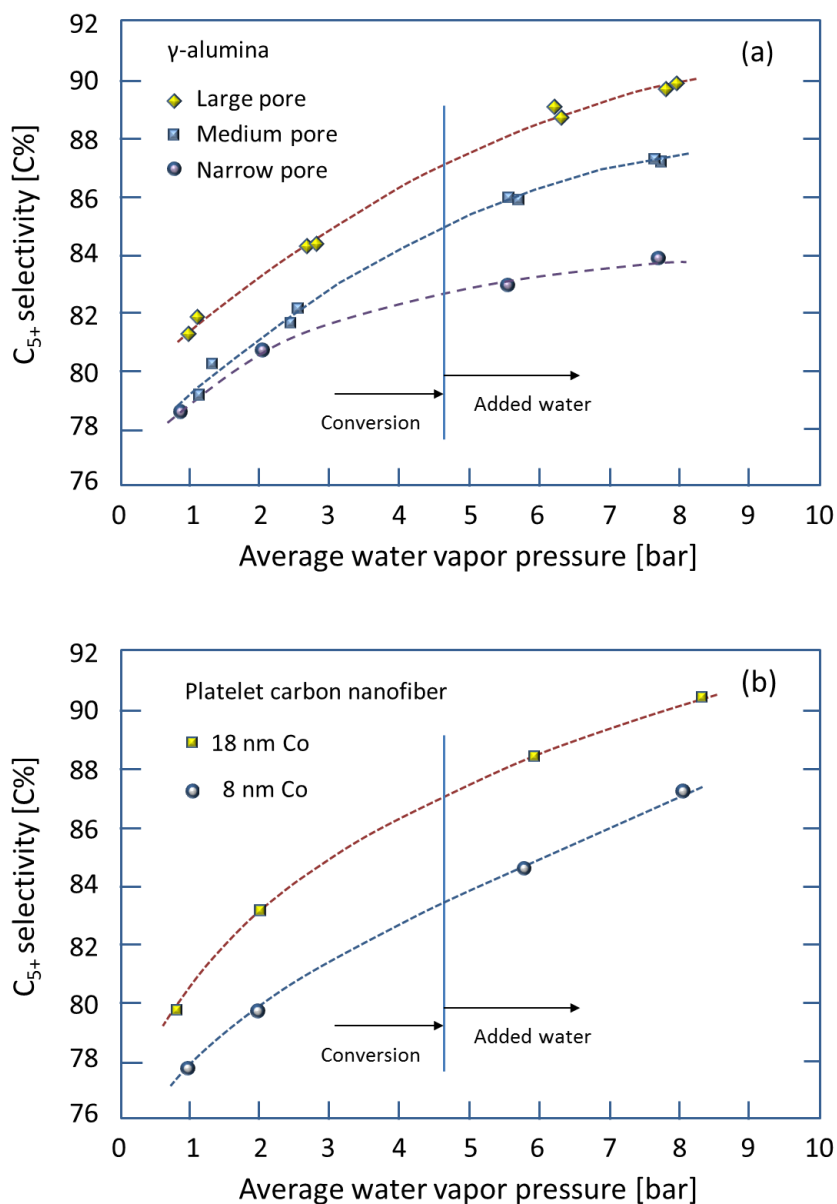


Figure 5.  $C_{5+}$  selectivity as a function of *in situ* generated and added water to feed in fixed-bed reactors. (a) 20 wt% Co/0.5 wt% Re on  $\gamma$ -alumina supports with different pore sizes; narrow pore: 184  $m^2/g$ , 7.4 nm; medium pore: 186  $m^2/g$ , 12.3 nm; wide pore: 155  $m^2/g$ , 20.8 nm. (b) Platelet carbon nanofiber; 18 and 8 nm Co crystallite size. Conditions: 210 °C; 20 bar;  $[H_2/CO]^0=2.1$ . Data collected from refs. 18 and 23, respectively.

It was pointed out in the introduction that most previous studies adopt a model whereby water promotes activation of CO with subsequent generation of  $CH_x$  monomer species that favors chain growth. It might be more challenging to explain why alumina with small pore size is relatively less efficient at high water vapor pressure levels. Dalai *et al.* demonstrated for silica based catalysts that the effect of water depends on the pore size of the support, much in line with the observations

for  $\gamma$ -alumina supports described above.<sup>30</sup> An explanation might be related to the observation that finely dispersed cobalt is susceptible to oxidation under these conditions as shown in several studies.<sup>31,32,33</sup> Oxidation might be promoted by surface condensation of water in narrow pores and on nano-scale support crystals. However, small Co crystallites generally result in suppressed  $C_{5+}$  selectivity, and removing these by oxidation then should enhance overall selectivity. On the other hand, some surface oxidation of larger Co crystallites has the opposite effect. In any case, more pronounced surface condensation of water in narrow pores, particularly at high water pressure levels, is a possible link to an explanation as enhanced bulk water vapor pressure then becomes less significant. To our knowledge, there has been no systematic study where the conditions deliberately have been varied to approach and exceed water condensation. Nevertheless, water condensation may explain the results in a study of a micro-channel reactor where  $C_{5+}$  selectivity as a function of CO conversion was studied at 20-40 bar and 210 and 225 °C.<sup>34</sup> It was unexpectedly found that the selectivity is lower at higher pressure at the lowest temperature; in line with water condensation and enhanced diffusion restrictions.

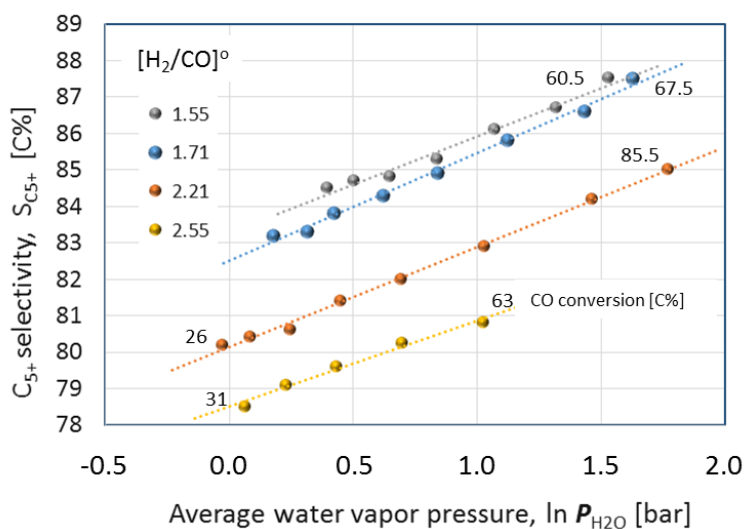


Figure 6.  $C_{5+}$  selectivity as a function of *in situ* generated water in fixed-bed reactors by stepwise increase of conversion. Conditions: 20wt% Co/0.5wt% Re/ $\gamma$ - $Al_2O_3$ ; 210 °C; 20 bar. Data from.<sup>35</sup>

A further dataset illustrating the effect on selectivity is shown in Figure 6 where the  $C_{5+}$  selectivity,  $S_{C_{5+}}$ , is plotted as a function of the water vapor pressure on a logarithmic scale for experiments with a number of different  $H_2/CO$  ratios in the feed of a fixed-bed reactor. The linear trendlines show that the effect of water on  $C_{5+}$  selectivity follows first order dependence in water vapor pressure. Further, the parallelism of the lines indicates a common cause of the displacement between them. In addition to water, it is obvious that the hydrogen partial pressure, as dictated here by the  $[H_2/CO]^0$  ratio for the four different series, is the main candidate to be explored. Indeed, plotting  $S_{C_{5+}}$  multiplied by an exponent of the partial pressure of hydrogen, instead of only  $S_{C_{5+}}$ , gives a horizontal trend line where all lines of Figure 6 collapse.

### Olefin selectivity and hydrogenation

Detection of light gas olefin to paraffin ratio is useful to elucidate pore diffusion as well as catalytic effects. Figure 7 illustrates how conversion and added water influence  $C_3$  olefin to paraffin ratio ( $o/p$ ) for cobalt on a medium to wide pore  $\gamma$ -alumina support during FTS.<sup>36</sup> It is reasonable that when water is added, the hydrogen partial pressure is reduced and the trendline is lifted due to less favorable conditions for secondary hydrogenation of olefins. In contrast, the effect of conversion is opposite and seemingly conflicting. However, this is due to the nature of consecutive reactions. As conversion is doubled by reducing space velocity, the increased time available for hydrogenation of olefins outweighs reduced partial pressure of hydrogen. Thus, the data are consistent with the prevailing mechanistic model of chain termination that yields olefins as the main primary product.<sup>36,37</sup>

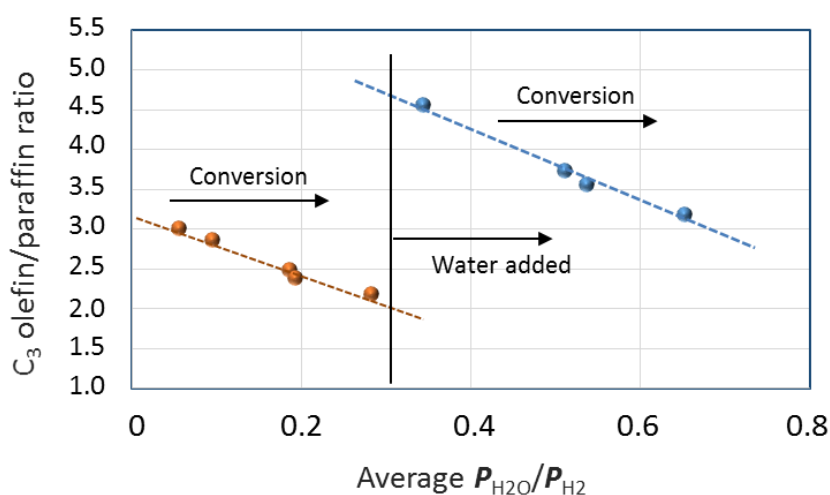


Figure 7.  $C_3$  olefin/paraffin ratio as a function of average water to hydrogen partial pressures for variations in conversion and water added to feed. Conditions: Co/Re/ $\gamma$ -alumina;  $H_2/CO=2.1$ ; 20 bar; 210 °C. Data from literature.<sup>36</sup>

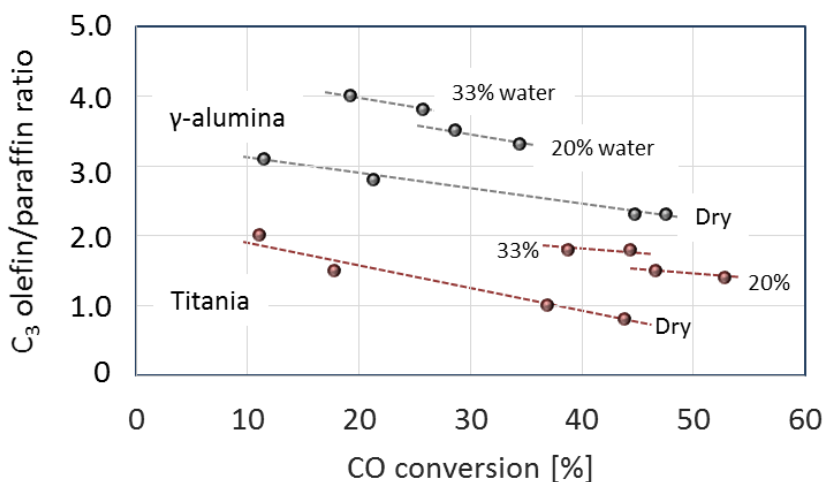


Figure 8.  $C_3$  olefin/paraffin ratio for Co and CoRe catalysts supported on titania and  $\gamma$ -alumina as a function of CO conversion and added water Conditions:  $H_2/CO=2.1$ ; 20 bar; 210 °C. Data from literature.<sup>23</sup>

Further evidence for the relationship between olefin hydrogenation, consecutive reactions and water content is shown in Figure 8 for cobalt catalysts on titania and  $\gamma$ -alumina. The same trends as in the previous figure are found for each support. In each pair of data points, the one at higher conversion is for catalyst promoted with rhenium at unchanged space velocity. Evidently, Re promotion does not alter the underlying mechanism for olefin hydrogenation and the response to water vapor pressure and residence time. Why titania evidently is a support that enhances olefin hydrogenation in spite of high selectivities to higher hydrocarbons, is a discussion beyond the present scope, but might be related to the well-known strong metal-support interaction and decoration of cobalt. The olefin/paraffin ratios increase consistently independent of chain length when water is added to the feed; see also Shi and Davis.<sup>37</sup> The effect of water on propene hydrogenation has also been studied separately and shows a very significant reduction in reaction rate.<sup>5</sup>

### Chain growth and methanation

Several examples of a one-to-one linear relationship between  $C_{5+}$  and  $CH_4$  selectivities have been shown previously. A prerequisite is that the temperature is constant, there are no syngas diffusion limitations, and the GHSV is adjusted to keep a constant CO conversion level. Examples encompasses Re and Ni promotion on different supports,<sup>21</sup> variations in Co-crystallite size on different transition aluminas,<sup>4,38,39</sup> effect of Ca-impurities,<sup>40</sup> and catalyst formulation and process conditions.<sup>41</sup> Here we demonstrate that this correlation is maintained in FTS when water is added to the syngas feed by plotting data from a high pressure steady-state isotopic transient kinetic analysis (SSITKA), see Figure 9.<sup>42</sup>

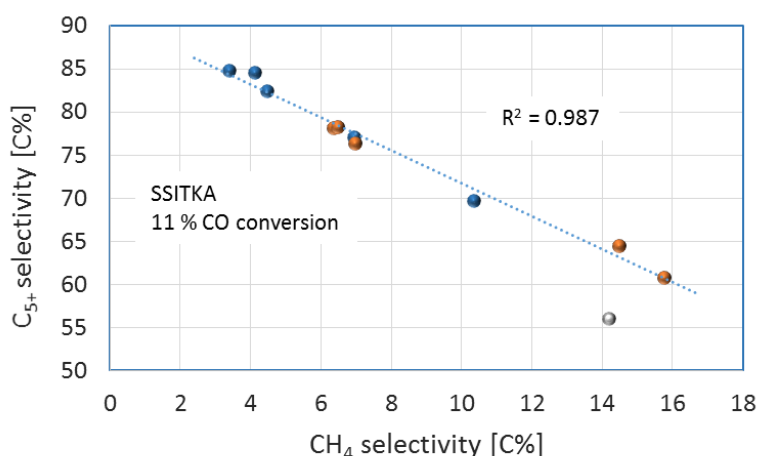


Figure 9. Selectivity to  $C_{5+}$  as function of selectivity to  $CH_4$  in SSITKA experiments at 11% CO conversion by varying the  $H_2/CO$  inlet ratio and adding steam (blue symbols). Assumption:

Outlier, without water addition, is exempted from trendline. Conditions: Unsupported Co-3 mol% Re catalyst, 210 °C; 3-15 bar syngas; H<sub>2</sub>/CO ratio 2-4; 0, 2, 4, 8 bar water added. Plotted from data in ref. 7.

It is frequently assumed that methane is formed in a parallel reaction to chain growth on separate sites and with its own rate determining step.<sup>43</sup> However, the straight line indicates a mechanistic link between all three fractions. Such a link is a common pool of CH<sub>x</sub> monomers that can shift composition between CH<sub>4</sub> prone; *i.e.* hydrogen rich CH<sub>x</sub>, or C<sub>5+</sub> prone; hydrogen lean CH<sub>x</sub>, according to conditions and catalyst formulation.<sup>4,10,19</sup>

### Mechanistic approach

The effect of water added to syngas in carbon isotope transient kinetic experiments at steady state was studied by Bertole *et al.*<sup>7</sup> Data for an unsupported Co-Re catalyst were obtained at 11% CO conversion and elevated pressures of syngas from 2-15 bar with added water at 2, 4 or 8 bar. In the four pairs with and without water addition, water in all cases increased the amount of active carbon (N<sub>C\*</sub>) on the cobalt surface. The concentration (N<sub>C\*</sub>/N<sub>CO</sub>) increased from 20 to 107%, most in the extreme case where nearly three times water was added to syngas and in the case where 40% water (4 bar) was added to syngas with a H<sub>2</sub>/CO ratio as high as 4. They deduced that water increases the amount of surface carbon, predominantly present as monomeric species, caused by acceleration of the CO dissociation rate. The high concentration of monomers, that we denote CH<sub>x</sub> pool, causes enhanced formation of high molecular weight FTS products and lower methane make.

The dominant products of Fischer-Tropsch synthesis are straight chain hydrocarbons; a mixture of alkanes and  $\alpha$ -olefins. Alkanes are mostly formed during secondary hydrogenation as discussed above, leaving  $\alpha$ -olefins as the main primary product. We do not consider olefin reinsertion in the growing chain,<sup>44</sup> as this mechanism has been shown to play a minor role.<sup>37,45,46</sup> There are several pathways for CO activation and monomer insertion that are being promoted in the literature; we select hydrogen assisted CO dissociation, followed by insertion of -CH<sub>x</sub> monomer units, as the most consistent mechanism.<sup>11,47,48,49,50</sup> From the above, a pathway for CO activation as illustrated in Figure 10 is based on the following steps:

- CO is activated by hydrogen attack on the carbon atom adsorbed to cobalt (the formyl route).
- The C-O bond is further weakened by H<sub>2</sub>O attack on the oxygen atom giving hydroxycarbene; \*HOCH\*
- Dissociation of \*HOCH\* is spontaneous providing CH\* as a methylidyne monomer (or alternatively hydrogen assisted through a second attack on carbon; providing a methylene monomer CH<sub>2</sub>\*).
- Finally, the adsorbed hydroxyl is hydrogenated and water can leave the surface.

The model is in reasonable agreement with published energies for CO activation on Ru by density functional theory (DFT).<sup>11</sup> Details of association to the surface will have to be established by

accurate quantum mechanical calculations, *e.g.* to what extent the oxygen of the formyl specie is interacting with cobalt. Thus, a consistent route for generation of propagation monomers from CO is



Water assisted CO activation to methylidyne

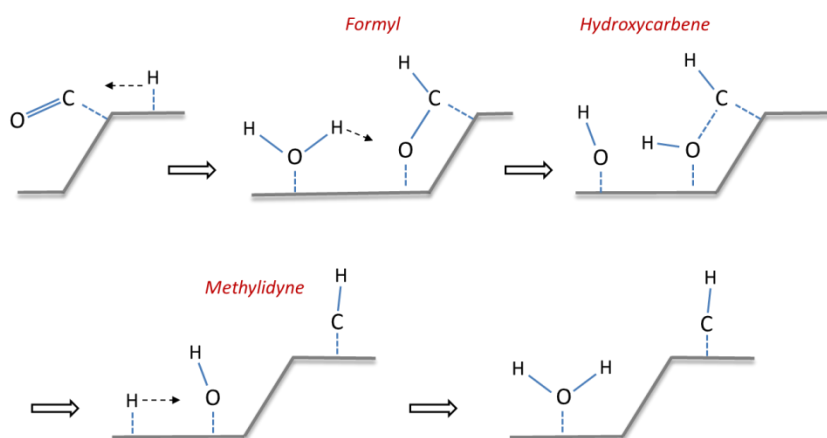
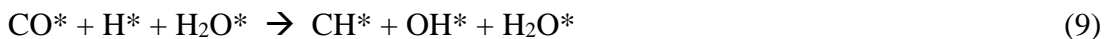


Figure 10. Suggested pathway for formation of  $\text{CH}^*$  monomers through water and hydrogen assisted dissociation of CO on cobalt step sites; the formyl route.

As water is a product of CO activation, it appears counterintuitive that water addition leads to higher catalyst activity. However, the key step is water activation of the oxygen atom through Eq. 6. It is feasible that hydrogen on water forms the well-established hydrogen bond with an adjacent oxygen atom; on the formyl specie to create hydroxycarbene,  $\text{*HOCH}^*$ . According to DFT calculations,<sup>11</sup> it is this step that has the highest activation barrier in the hydrogen assisted formyl route and needs to be brought down. The authors have considered several mechanisms for hydrogen transfer from water on ruthenium and favors “route with  $\text{H}_2\text{O}$  as solvent or H-shuttle”. In this case water in the gas phase picks up a hydrogen atom from the metal surface and transfers it to oxygen of CO. Saeys and co-workers proposed a similar mechanism, but used hydroxyl to provide hydrogen attack on the formyl oxygen atom.<sup>51</sup> There is another apparently trivial difference between the two models represented by Eqs. 7a and 7b above; the first scheme with direct hydroxycarbene dissociation produces methylidyne,  $\text{CH}^*$ , as a possible primary chain

building block.<sup>51,52</sup> This implies that after CH\* insertion, the growing chain picks up a hydrogen atom to give -CH<sub>2</sub>-, thus completing a saturated alkyl group.

Activation can be written in a concerted form as



Subsequently, the primary CH\* monomer is subject to hydrogenation;



which creates the CH<sub>x</sub> pool on cobalt:



That water promotes chain growth is simply because enhanced activation provides a higher concentration of monomers on the metal surface without commensurate effect on chain termination,<sup>4,7,53</sup> Previously, we also proposed that water/hydroxyl suppresses hydrogen chemisorption and shifts the CH<sub>x</sub> pool towards chain growth in expense of methanation. Olefin hydrogenation, as well as termination by chain end hydrogenation, are suppressed as well. The proposed reaction network is in accordance with most experimental responses to water discussed above and to the interplay between hydrogen and water on the active cobalt surface. A prerequisite is that narrow pore systems and very high water concentrations are exempt, possibly due to water condensation and/or cobalt oxidation.<sup>19</sup>

## Conclusions

It has been shown that water can be both positive and negative for Fischer-Tropsch synthesis depending on the conditions, in particular the gas composition. There are positive correlations of catalyst activity with water concentration for most catalysts and of C<sub>5+</sub> selectivity for all types of catalysts. There are indications that condensation of water occurs in small pores and, more generally, under close to bulk water condensation conditions, but this hypothesis requires further studies. Further, there is limited understanding of mechanistic aspects of water, although water induced promotion of CH<sub>x</sub> monomers has been inferred. There is specifically no study where there are controlled variations of cobalt crystallite size and water concentration. A further implication and complication of water in FTS is that kinetic expressions depend on the catalyst formulation, meaning that no general Fischer-Tropsch reaction rate law exists. For both slurry and fixed-bed reactor types, understanding and controlling water level is a key to successful operation during Fischer-Tropsch synthesis.

## Notes

The authors declare no financial interest

## References

- <sup>1</sup> Blekkan, E. A.; Borg, Ø.; Frøseth, V.; Holmen, A. *Catal., Royal Soc. Chem.* **2007**, *20*, 13-32.
- <sup>2</sup> Hilmen, A. M.; Lindvåg, O. A.; Bergene, E.; Schanke, D.; Eri, S.; Holmen, A. *Stud. Surf. Sci. Catal.* **2001**, *136*, 295-300.
- <sup>3</sup> Friedel, R. A.; Anderson, R. B. *J. Am. Chem. Soc.* **1950**, *72*, 1212-1215.
- <sup>4</sup> Rytter, E.; Tsakoumis, N. E.; Holmen, A. *Cat. Today* **2016**, *261*, 3-16.
- <sup>5</sup> Aaserud, C.; Hilmen, A.-M.; Bergene, E.; Eri, S.; Schanke, D.; Holmen, A. *Catal. Lett.* **2004**, *94*, 171-176.
- <sup>6</sup> Krishnamoorthy, S.; Tu, M.; Ojeda, M. P.; Pinna, D.; Iglesia, E. *J. Catal.* **2002**, *211*, 422-423.
- <sup>7</sup> Bertole, C. J.; Mims, C. A.; Kiss, G. *J. Catal.* **2004**, *221*, 191-203.
- <sup>8</sup> Iglesia, E. *Appl. Catal. A* **1997**, *161*, 59-78.
- <sup>9</sup> Fischer, N.; Clapham, B.; Feltes, T.; Claeys, M. *Catal.* **2015**, *5*, 113-121.
- <sup>10</sup> Lögdberg, S.; Lualdi, M.; Järås, S.; Walmsley, J. C.; Blekkan, E. A.; Rytter, E.; Holmen, A. *J. Catal.* **2010**, *274*, 84-98.
- <sup>11</sup> Hibbitts, D. D.; Loveless, B. T.; Neurock, M.; Iglesia, E. *Ang. Chem. Int. Ed.* **2013**, *52*, 12273-12278.
- <sup>12</sup> Qi, Y. *Mechanistic Insights into Cobalt-based Fischer-Tropsch Synthesis*, Ph.D. thesis NTNU 2016-106, 2016.
- <sup>13</sup> Rytter, E.; Holmen, A. *Catalysts* **2015**, *5*(2), 478-499.
- <sup>14</sup> Twigg, M. W. ed., *Catalyst Handbook*, 2<sup>nd</sup> ed., Wolfe Publishing, London, 1989.
- <sup>15</sup> Coronado, I.; Stekrova, M.; Reinikainen, M.; Simell, P.; Lefferts, L.; Lehtonen, J. *Int. J. Hydrogen En.* **2016**, *41*, 11003-11032.
- <sup>16</sup> Bezemer, G. L.; Nkrumah, S.; Smits, J. T. M. *patent* US 2012/0165417.
- <sup>17</sup> Leviness, S. *245th ACS National Meeting*, April 2013, New Orleans.  
[http://www.velocys.com/arcv/press/ppt/ACS%202013%20Presentation%2004-09-13%20-%20FINAL\\_rev1.pdf](http://www.velocys.com/arcv/press/ppt/ACS%202013%20Presentation%2004-09-13%20-%20FINAL_rev1.pdf)
- <sup>18</sup> Borg, Ø.; Storsæter, S.; Eri, S.; Wigum, H.; Rytter, E.; Holmen, A. *Catal. Lett.* **2006**, *107*, 95-102.
- <sup>19</sup> Rytter, E.; Holmen, A. *Catal. Today* **2016**, *275*, 11-19.
- <sup>20</sup> Enger, B. C.; Fossan, Å.-L.; Borg, Ø.; Rytter, E.; Holmen, A. *J. Catal.* **2011**, *284*, 9-22.
- <sup>21</sup> Rytter, E.; Skagseth, T.H.; Eri, S.; Sjøstad, A.O. *Ind. Eng. Chem. Res.* **2010**, *49*, 4140.
- <sup>22</sup> Storsæter, S.; Borg, Ø.; Blekkan, E.A.; Holmen, A. *J. Catal.* **2005**, *231*, 405-419.
- <sup>23</sup> Borg, Ø.; Yu, Z.; Chen, D.; Blekkan, E. A.; Rytter, E.; Holmen, A. *Top. Catal.* **2014**, *57*, 491-499.
- <sup>24</sup> Ma, W.; Jacobs, G.; Sparks, D.E.; Spicer, R.L.; Davis, B.H.; Klettlinger, J.L.S.; Yen, C.H. *Catal. Today* **2014**, *228*, 158-166.
- <sup>25</sup> Withers Jr, H.P.; Eliezer, K.F.; Mitchel, J.M. *Ind. Eng. Chem. Res.* **1990**, *29*, 1807-1814.
- <sup>26</sup> van Steen, E.; Schulz, H. *Appl. Catal. A* **1999**, *186*, 309-320.
- <sup>27</sup> Das, T.K.; Conner, W.A.; Li, J.; Jacobs, G.; Dry, M.E.; Davis, B.H. *Energy Fuels* **2005**, *10*, 1430-1439.
- <sup>28</sup> Bhatelia, T.; Ma, W.; G. Jacobs; Davis, B.H.; Bukur, D.B. *Chem. Eng. Trans.* **2011**, *25*, 707-712.
- <sup>29</sup> M. Ostadi, E. Rytter, M. Hillestad, *Chem. Eng. Res. Design* **2016**, *114*, 236-246.
- <sup>30</sup> Dalai, A.K.; Das, T.K.; Chaudhari, K.V.; Jacobs, G.; Davis, B.H.; *Appl. Catal. A* **2005**, *289*, 135-142.
- <sup>31</sup> Schanke, D.; Hilmen, A.-M.; Bergene, E.; Kinnari, K.; Rytter, E.; Ådnanes, E.; Holmen, A. *Catal. Lett.* **1995**, *34*, 269-284.
- <sup>32</sup> van Berge, P.; van de Loosdrecht, J.; Barradas, S.; van der Kraan, A. *Catal. Today* **2000**, *58*, 321-324.
- <sup>33</sup> van Steen, E.; Claeys, M.; Dry, M.E.; van de Loosdrecht, J.; Viljoen, E.L.; Visagie, J.L. *J. Phys. Chem B* **2005**, *109*, 3575-3577.
- <sup>34</sup> Yang, J.; Eiras, S.B.; Myrstad, R.; Pfeifer, P.; Venvik, H.J.; Holmen, A. In *Fischer-Tropsch Synthesis, Catalysts, and Catalysis*, Eds.: B.H. Davis, M.L. Occelli. CRC Press, Taylor & Francis Group, Chemical Industries/142 Chap 12, p 223 (2016)
- <sup>35</sup> Holmen, A.; Lillebø, A.H.; Rytter, E.; Blekkan, E.A. Submitted to *Ind. Eng. Chem. Res.* 2017.



- 
- <sup>36</sup> Rytter, E.; Eri, S.; Skagseth, T.H.; Schanke, D.; Bergene, E.; Myrstad, R.; Lindvåg, A. *Ind. Eng. Chem. Res.* **(2007)** *46*, 9032-9036.
- <sup>37</sup> Shi, B.; Davis, B.H. *Catal. Today* **2005**, *106*, 129-131.
- <sup>38</sup> Borg, Ø.; Dietzel, P.D.C.; Spjelkavik, A.I.; Tveten, E.Z.; Walmsley, J.C.; Diplas, S.; Eri, S.; Holmen, A.; Rytter, E. *J. Catal.* **2008**, *259*, 161-164.
- <sup>39</sup> Rane, S.P.; Borg, Ø.; Rytter, E.; Holmen, A. *Appl. Catal. A: Gen.* **2012**, *437-438*, 10-17.
- <sup>40</sup> Borg, Ø.; Hammer, N.; Enger, B.C.; Myrstad, R.; Lindvåg, O.A.; Eri, S.; Skggseth, T.H.; Rytter, E. *J. Catal.* **2011**, *279*, 163-173.
- <sup>41</sup> Løgdberg, S.; Lualdi, M.; Järås, S.; Walmsley, J.C.; Blekkan, E.A.; Rytter, E.; Holmen, A. *J. Catal.* **2010**, *274*, 84-98.
- <sup>42</sup> Bertole, C.J.; Mims, C.A.; Kiss, G. *J. Catal.* **2002**, *210*, 84-96.
- <sup>43</sup> Schulz, H.; Nie, Z.; Ousmanov, F. *Catal. Today* **2002**, *71*, 351-360.
- <sup>44</sup> Schulz, H.; Claeys, M. *Appl. Catal.* **1990**, *186*, 91-107.
- <sup>45</sup> Patzlaff, J.; Liu, Y.; Craffmann, C.; Gaube, J. *Catal. Today* **2002**, *71*, 381-394.
- <sup>46</sup> Borg, Ø.; Eri, S.; Blekkan, E.A.; Storsæter, S.; Wigum, H.; Rytter, E.; Holmen, A. *J. Catal.* **2007**, *248*, 89-100.
- <sup>47</sup> Vannice, M. *Catal. Rev. Sci. Eng.* **1976**, *14*, 153-191.
- <sup>48</sup> Iglesia, E.; Reyes, S.; Madon, R.; Soled, S. *Adv. Catal.* **1993**, *39*, 221-302.
- <sup>49</sup> Storsæter, S.; Chen, D.; Holmen, A. *Surf. Sci.* **2006**, *600*, 2051-2063.
- <sup>50</sup> Yang, J.; Qi, Y.; Zhu, J.; Zhu, Y.A.; Zhu, D.; Chen, D.; Holmen, A. *J. Catal.* **2013**, *308*, 37-49.
- <sup>51</sup> Gunasooriya, G.T.K.K.; van Bavel, A.P.; Kuipers, H.P.C.E.; Saeys, M. *ACS Catal.* **2016**, *6*, 3660-3664.
- <sup>52</sup> Weststrate, C.J.; Ciobîcă, I.M.; Saib, A.M.; Moodley, D. J.; Niemantsverdriet, J. W. *Catal. Today* **2014**, *228*, 106-112.
- <sup>53</sup> Bertole, C.J.; G. Kiss, G.; C.A. Mims, C.A. *J. Catal.* **2004**, *223*, 309-318.

---

**ACS Catalysis**  
Msc: cs7b01525

The following graphic will be used for the TOC:

Water assisted CO activation to methylidyne

